

DSP Based Simulator for Field Oriented Control of the Surface Permanent Magnet Synchronous Motor Drive

Abdel-Karim Daud, Basim Alsayid, Arafat Zaidan

Abstract-- Permanent Magnet Synchronous Motors (PMSM) have wide applications in industry, especially in AC servo drives. Digital Signal Processors (DSP) has greatly enhanced the potential of PMSM servo drive in such applications. Most of controller drives the PMSM by using the field-orientation control mode. This method laid the motor at maximum theoretical performance.

This paper presents the field oriented vector control scheme for permanent magnet synchronous motor (PMSM) drives, where current controller followed by hysteresis comparator is used. The field oriented vector control, that regulates the speed of the PMSM, is provided by a quadrature axis current command developed by the speed controller. The simulation includes all realistic components of the system. This enables the calculation of currents and voltages in different parts of the voltage source inverter (VSI) and motor under transient and steady state conditions. Implementation has been done in MATLAB/Simulink. A study of hysteresis control scheme associated with current controllers has been made. Experimental results of the PMSM control using TMS320F24X DSP board are presented. The speed of the PMSM is successfully controlled in the constant torque region.

Experimental results show that the PMSM exhibits improved speed stability especially in very low speed range. The validity and usefulness of the proposed control scheme are verified through simulation and experimental results.

Keywords-- Field Oriented Control, PMSM, Hysteresis Current Controller, DSP, MATLAB/Simulink

I. INTRODUCTION

PERMANENT magnet (PM) synchronous motors are widely used in low and mid power applications such as computer peripheral equipments, robotics, adjustable speed drives, electric vehicles and other applications in a variety of automated industrial plants. In such applications, the motion controller may need to respond relatively swiftly to command changes and to offer enough robustness against the uncertainties of the drive system [2, 4, 7, 8]. Among ac and dc drives, PMSM has received widespread appeal in motion control applications.

Abdel-Karim Daud is with Electrical and Computer Engineering Department Palestine Polytechnic University (PPU), P.O. Box 198 Hebron, Palestine, (Tel: +972-2-2228912, Fax: +972-2-2217248; e-mail: daud@ppu.edu).

Alsayid Basim is with Electrical Engineering Department, Palestine Technical University (PTU), P.O. Box 7 Tulkarm, Palestine, (Tel: +972-9-2688175, Fax: +972-2-2677922; e-mail: basimbo@yahoo.com).

Arafat Zaidan is with Electrical Engineering Department, Palestine Technical University (PTU), P.O. Box 7 Tulkarm, Palestine, (Tel: +972-9-2688175, Fax: +972-2-2677922; e-mail: arafatzaidan@yahoo.co.uk).

The complicated coupled nonlinear dynamic performance of PMSM can be significantly improved using vector control theory [3, 4, 5, 7, 9, 10] where torque and flux can be controlled separately.

The growth in the market of PM motor drives has demanded the need of simulation tools capable of handling motor drive simulations.

Under perfect field orientation and with constant flux operation, a simple linear relation can characterize the torque production in the motor when the magnetic circuit is linear [11, 12, 13, 14, 15-22].

However, the control performance of PMSM drive is still influenced by uncertainties, which usually are composed of unpredictable plant parameter variations, external load disturbances, and unmodeled and nonlinear dynamics of the plant.

Simulations have helped the process of developing new systems including motor drives, by reducing cost and time. Simulation tools have the capabilities of performing dynamic simulations of motor drives in a visual environment so as to facilitate the development of new systems [6, 15].

In this work, the simulation of a field oriented controlled PM motor drive system is developed using MATLAB/Simulink. The simulation circuit will include all realistic components of the drive system. This enables the calculation of currents and voltages in different parts of the inverter and motor under transient and steady state conditions. A closed loop control system with a PI controller in the speed loop has been designed to operate in constant torque region. A study of hysteresis control scheme associated with current controller has been made. Simulation results are given for the speed range in constant torque region of motor operation. Finally, the experimental verification obtained by using the DSP based vector control is presented.

II. PMSM DRIVE SYSTEM

A. Modeling of PMSM

PMSM is composed of three phase's stator windings and permanent magnets mounted on the rotor surface (surface mounted PMSM) or buried inside the rotor (interior PMSM). It means that the excitation flux is set-up by magnets; subsequently no magnetizing current is needed from the supply.

The electrical equations of the PM synchronous motor can be described in the rotor rotating reference frame, written in the (dq) rotor flux reference frame [11, 13, 15-22].

The mathematic model of PMSM is based on the following assumptions:

- (1) Neglecting the saturation of armature;
- (2) Neglecting the wastages of eddy and magnetic hysteresis;
- (3) There is no rotor damp resistance.

The relations of voltage, torque and flux of surface mounted PMSM are described as follows:

$$\frac{d}{dt} \begin{bmatrix} i_q \\ i_d \end{bmatrix} = \begin{bmatrix} -R/L & -\omega_r \\ \omega_r & -R/L \end{bmatrix} \begin{bmatrix} i_q \\ i_d \end{bmatrix} + \begin{bmatrix} 1/L & 0 & 0 \\ 0 & 1/L & -\omega_r/L \end{bmatrix} \begin{bmatrix} v_q \\ v_d \\ \lambda_f \end{bmatrix} \quad (1)$$

where i_d and i_q are the d and q axis stator currents, R and L are the stator phase resistance and inductance respectively; the d -axis self inductance (L_d) and the q -axis self inductance (L_q) are all equal to L ; ω_r is the rotor electrical speed; v_d and v_q are the stator voltages expressed in the dq reference frame and λ_f is the flux linkage established by rotor permanent magnets.

The inverter frequency is related as follows

$$\omega_s = P \omega_r \quad (2)$$

where P is the number of pole pairs.

The electromagnetic torque is given by

$$T_e = \frac{3}{2} P [\lambda_f i_q + (L_d - L_q) i_d i_q] \quad (3)$$

The basic principle in control of PMSM drive is based on field orientation. The flux position can be determined by the shaft position sensor because the magnetic flux generated by permanent magnet is fixed in relation to the rotor shaft position. To ensure the vector control of the PMSM, the technique $i_d=0$ is the optimal strategy where the motor produce the maximum torque. If i_d is forced to be zero by closed loop control, then:

$$T_e = k_t i_q \quad (4)$$

with

$$k_t = \left(\frac{3}{2}\right) P \lambda_f \quad (5)$$

Since λ_f is constant, the electromagnetic torque is then directly proportional to current i_q . The torque equation is similar to that of separated excited DC motor. This feature can simplify the controller design of the PMSM, which is used in the controller simulation experiment in this paper.

The equation of the motor dynamics is

$$T_e = T_L + B \omega_r + J (d\omega_r/dt) \quad (6)$$

T_L stands for external load torque. B represents the damping coefficient and J is the moment of inertia of the rotor.

It is evident from equations (4) and (6) that the speed control can be achieved by controlling the q -axis current component i_q as long as the d -axis current i_d is maintained at zero.

The equations (1) and (6) constitute the whole control model of the PMSM.

A system configuration of a vector-controlled PMSM drive system is shown in Fig. 1.

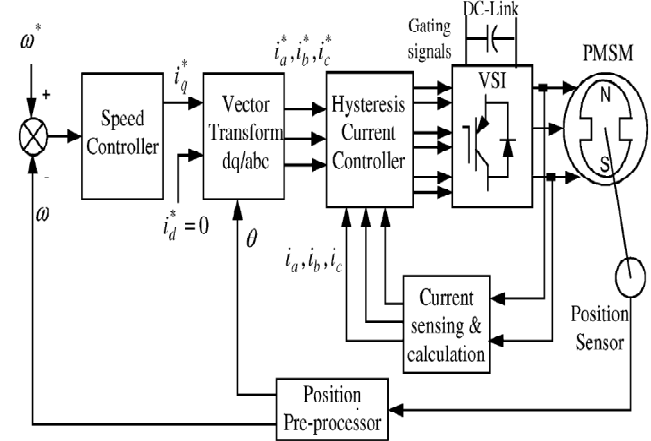


Fig.1 PMSM vector-controlled drive with constant flux operation

B. Vector Transformation dq/abc

The dynamic dq modeling is used for the study of motor during transient and steady state. It is done by converting the dqo variables to three phase currents by using inverse Parks transformation [11, 13, 15-22].

Converting the phase currents variables i_{dqo}^* to i_{abc}^* variables in rotor reference frame the following equations are obtained

$$\begin{bmatrix} i_a^* \\ i_b^* \\ i_c^* \end{bmatrix} = \begin{bmatrix} \cos\theta & \sin\theta & 1 \\ \cos(\theta - 120) & \sin(\theta - 120) & 1 \\ \cos(\theta + 120) & \sin(\theta + 120) & 1 \end{bmatrix} \begin{bmatrix} i_q^* \\ i_d^* \\ i_o^* \end{bmatrix} \quad (7)$$

C. Current Controlled Inverter

PMSM is fed from a voltage source inverter (VSI) with current control. The control is performed by regulating the flow of current through the stator of the motor. Current controllers are used to generate gate signals for the inverter. Proper selection of the inverter devices and selection of the control technique will guarantee the efficiency of the drive.

Voltage Source Inverter (VSI)

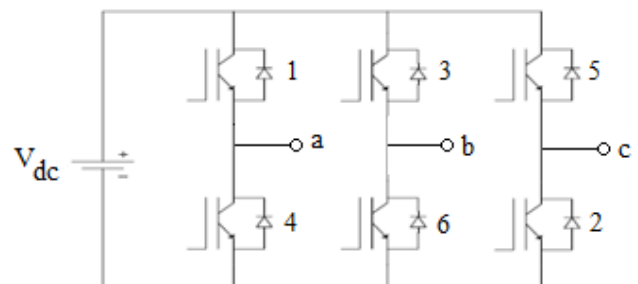


Fig. 2 Voltage source inverter (VSI)

Voltage Source Inverters (VSI) are devices that convert a DC voltage to AC voltage of variable frequency and magnitude. They are very commonly used in adjustable speed drives and are characterized by a well defined switched voltage wave form in the terminals [1, 13].

Fig. 2 shows a voltage source inverter. Three phase inverters consist of six power switches connected as shown in Fig. 2 to a DC voltage source. The inverter switches must be carefully selected based on the requirements of operation, ratings and the application. There are several devices available today and these are thyristors, bipolar junction transistors (BJTs), MOS field effect transistors (MOSFETs), insulated gate bipolar transistors (IGBTs) and gate turn off thyristors (GTOs). MOSFETs and IGBTs are preferred by industry because of the MOS gating permits high power gain and control advantages. While MOSFET is considered a universal power device for low power and low voltage applications, IGBT has wide acceptance for motor drives and other application in the low and medium power range. The power devices when used in motor drives applications require an inductive motor current path provided by antiparallel diodes when the switch is turned off.

Hysteresis Regulator

In the vector control scheme, torque control can be carried out by suitable regulation of the stator current vector; this implies that accurate speed control depends on how well the current vector is regulated. In high-performance vector drives, a current-control loop, with a considerably high bandwidth, is necessary to ensure accurate current tracking, to shorten the transient period as much as possible and to force the voltage source inverter (VSI) to equivalently act as a current source amplifier within the current loop bandwidth. In this work, a hysteresis-band current controlled VSI is used. To achieve a regular switching frequency and low harmonic content in the stator currents, a band hysteresis current controller is used.

This controller will generate the reference currents with the inverter within a range which is fixed by the width of the band gap. In this controller the desired current of a given phase (i_a^* , i_b^* and i_c^*) is summed with the negative of the measured current (i_a , i_b and i_c). When the current error exceeds a predefined hysteresis band, the upper switch in the half-bridge is turned off and the lower switch is turned on. As the current error goes below the hysteresis band, the opposite switching takes place. The principle of hysteresis band current control is illustrated in Fig. 3.

Peak to peak current ripple and switching frequency are related to the width of hysteresis band. As the width of the hysteresis band increases, the current ripples increases and the switching frequency decreases. On the other hand when the hysteresis band decreases, the current waveform becomes better having less low order harmonic contents but in this case the switching frequency increases and consequently the switching losses. As a result, the selection of the width of the hysteresis band must be carried out to optimize the balance between harmonic ripples and inverter switching losses.

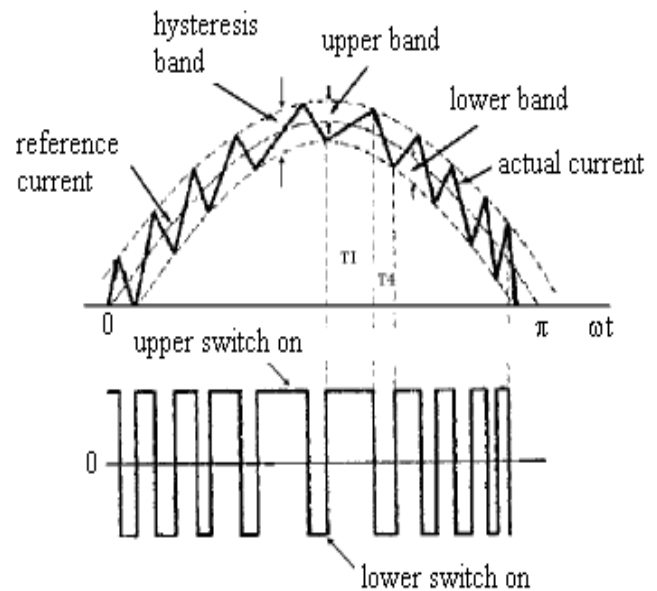


Fig.3 Hysteresis current controller

Hysteresis-band current control is very popular because it is simple to implement, has fast transient response, direct limiting of device peak current and practical insensitivity to machine parameters because of the elimination of any additional current controllers. However, PWM frequency is not fixed which results in non-optimal harmonic ripple in machine current.

This controller does not have a specific switching frequency and changes continuously but it is related with the band width [13, 15, 23-24].

D. Implementation of the Speed Control Loop

Speed controller calculates the difference between the reference speed (ω^*) and the actual speed (ω) producing an error, which is fed to the PI controller. PI controllers are used widely for motion control systems. Speed control of motors mainly consist of two loops the inner loop for current (band hysteresis current controller) and the outer loop for speed (speed controller) as shown in Fig.1. The order of the loops is due to their response, how fast they can be changed. This requires a current loop at least 10 times faster than the speed loop.

An optical encoder is used as a position sensor, which consists of a rotating disk, a light source, and a photo detector (light sensor) as shown in Fig. 4. The disk, is mounted on the rotating shaft, has coded patterns of opaque and transparent sectors. As the disk rotates, these patterns interrupt the light emitted onto the photo detector, generating a digital pulse or output signal. Optical encoders offer the advantages of digital interface.

One type of optical encoders is called an incremental encoder, which is used in this system. Incremental encoders have good precision and are simple to implement. The most common type of incremental encoder uses two output channels (A and B) to sense position.

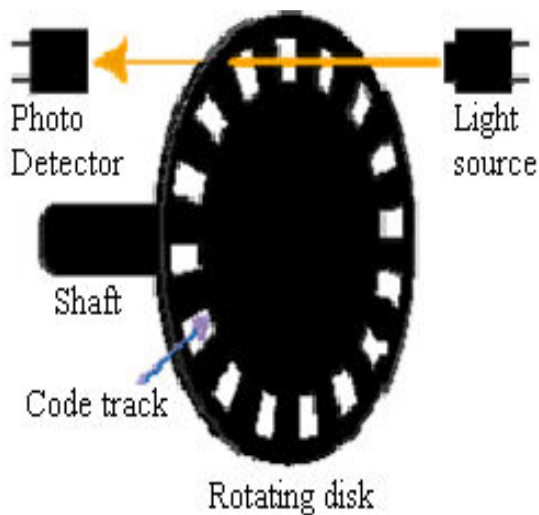


Fig. 4 Optical encoder

Using two code tracks with sectors positioned 90° degrees out of phase, the two output channels of the quadrature encoder indicate both position and direction of rotation as shown in Fig. 5. If A leads B, for example, the disk is rotating in a clockwise direction. If B leads A, then the disk is rotating in a counter-clockwise direction. By monitoring both, the number of pulses and the relative phase of signals A and B, it's possible to track position and direction of rotation. Some quadrature encoders also include a third output channel, called a zero or index or reference signal, which supplies a single pulse per revolution. This single pulse is used for precise determination of a reference position. The precision of the encoder is fixing by its code disk but it can be increased by detecting the Up and Down transitions on both the A and B channels.

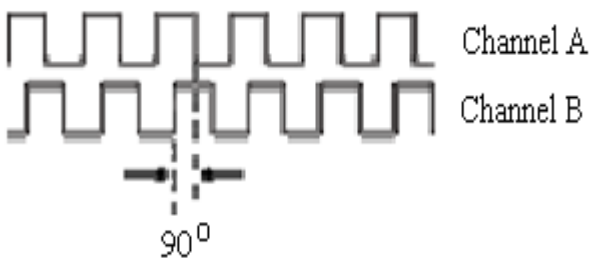
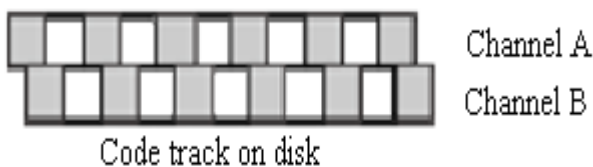


Fig. 5 Quadrature Encoder Channels

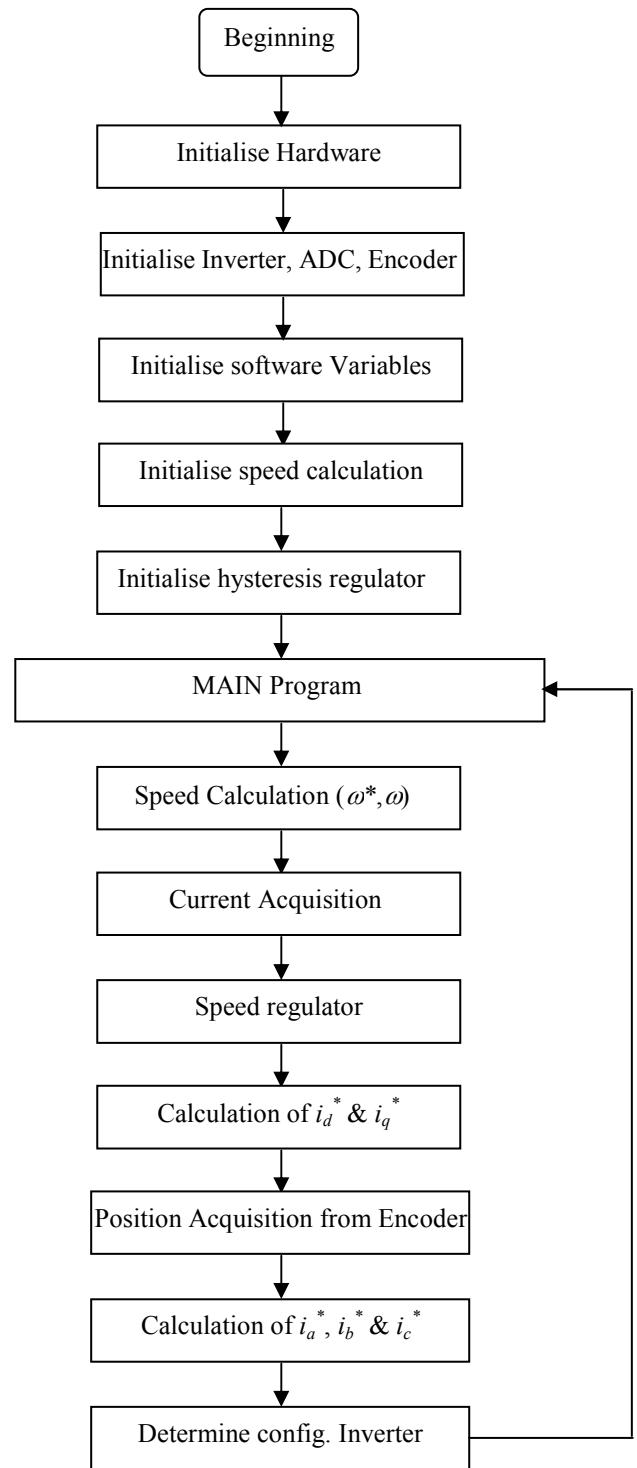


Fig. 6 System Flow Diagram

E. Software Implementation

Control loops in the actual drive system, shown in Fig. 1, are implemented in software on Texas Instruments (TMS320F24X) processor and executed with a cycle period of $70\mu\text{s}$. The flow-chart of this program is shown in Fig. 6. At switching on, the program initialises the hardware registers, I/O ports are then pre-set to their initial states, the inverter, ADC converters, position sensor (optical encoder) and software variables. Then it initialises the speed calculation and hysteresis regulators. The system now completes all initialisations and starts the main program which requires a computational time of $70\mu\text{s}$ of period cycle.

The main program will first calculate actual speed of the motor (ω), read reference speed (ω^*) and actual currents (i_a , i_b and i_c) from ADCs. Errors are then saved and new errors are calculated. Speed regulator is realised by a discrete PI. Calculation of i_q^* and i_d^* in the rotating reference frame is done. Then it will read position from the encoder. Based on rotor position, three-phase reference currents (i_a^* , i_b^* and i_c^*) in the stationary reference frame are calculated. This is followed by the execution of currents loop and resulting controlled signals are sent to the inverter.

III. SIMULATION IN SIMULINK

Simulink has the advantages of being capable of complex dynamic system simulations, graphical environment with visual real time programming and broad selection of tool boxes [11]. The simulation environment of Simulink has a high flexibility and expandability which allows the possibility of development of a set of functions for a detailed analysis of the electrical drive. Its graphical interface allows selection of functional blocks, their placement on a worksheet, selection of their functional parameters interactively, and description of signal flow by connecting their data lines using a mouse device. System blocks are constructed of lower level blocks grouped into a single maskable block. Simulink simulates analogue systems and discrete digital systems [24].

The PMSM drive simulation was built in several steps like dqo variables transformation to abc phase, calculation torque and speed, control circuit, inverter and PMSM. The dqo variables transformation to abc phase is built using the reverse Parks transformation. For simulation purpose the voltages are the inputs and the current are output. Using all

the drive system blocks, the complete system block has been developed as shown in Fig.7.

The system built in Simulink for a PMSM drive system has been tested with the Hysteresis current control method at the constant torque region of operation.

The motor parameters used for simulation are given in Table 1.

Name	Symbol	Value
Rated power	P_n	3.9 kW
Rated voltage	V_n	180 V
Rated torque	T_n	12.5 N·m
pull out torque	T_{max}	45 N·m
Rated current	I_n	14.9 A
Rated speed	n_n	3000 RPM
Number of pole pairs	P	3
Stator resistance	R_s	0.3 Ω
PM flux linkage	λ_f	0.185 Wb
q-axis Inductance	L_q	0.0085 H
d-axis Inductance	L_d	0.0085 H
Motor Inertia	J	0.0755 kgm ²

Table 1: PMSM Parameters

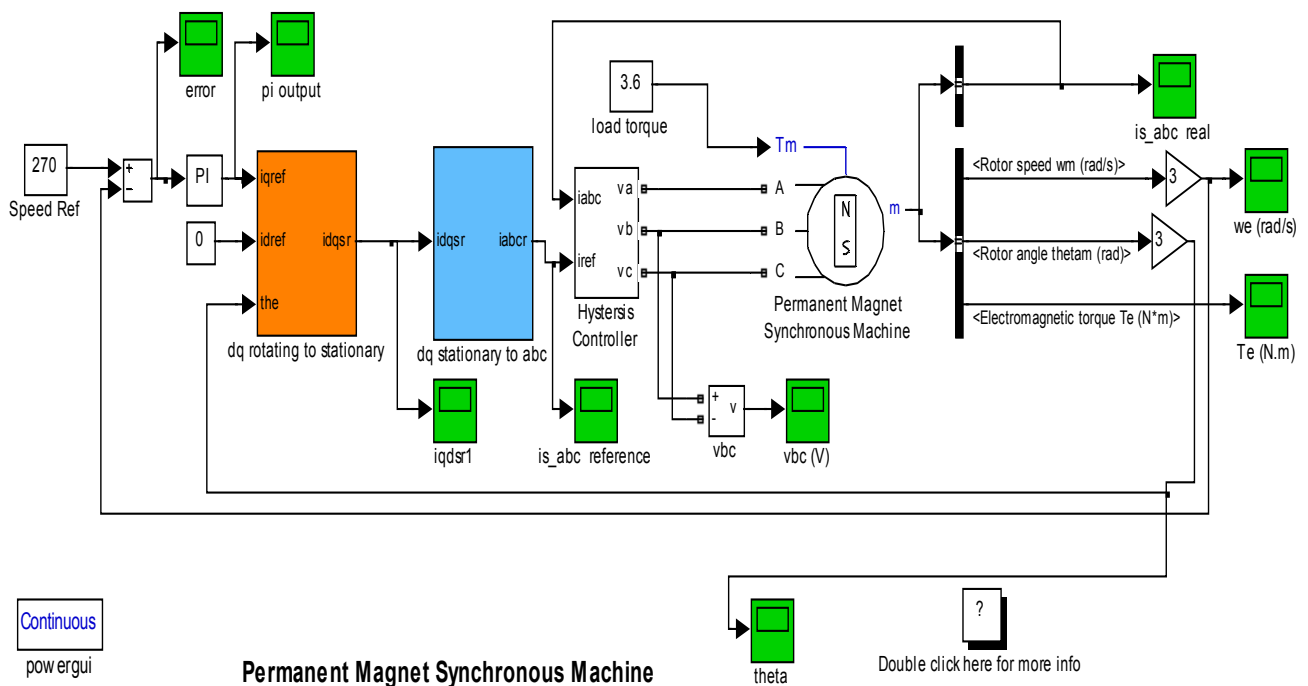


Fig. 7: PM Synchronous Motor Drive System in Simulink

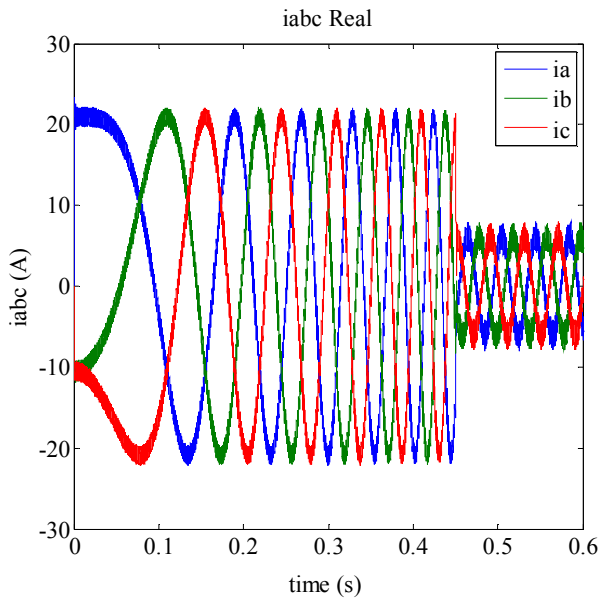


Fig. 8: Actual phase currents with Hysteresis Control at 1500 rpm rad/s

Fig. 8 shows the real three phase currents drawn by the motor as a result of the hysteresis current control, where the comparison between the actual and desired current for phase a is displayed in Fig. 9. The currents are obtained using Park's reverse transformation. It is clear that the current is non sinusoidal at the starting and becomes sinusoidal when the motor reaches the controller command speed at steady state.

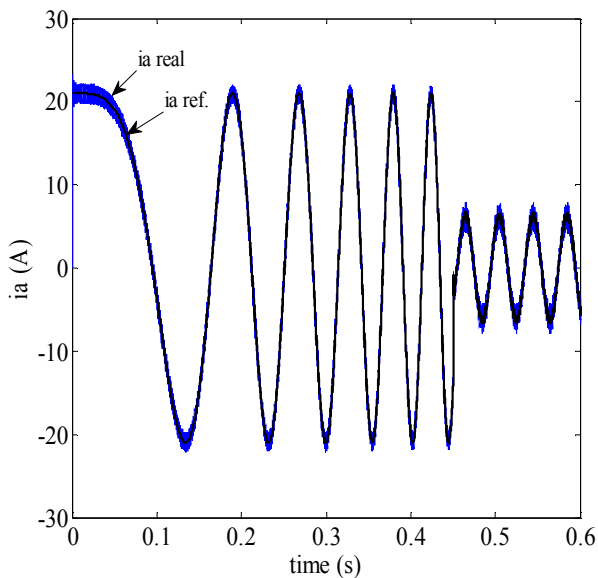


Fig. 9: Actual and desired current for phase at 1500 rpm rad/s

Fig. 10 shows a variation of the speed with time. The steady state speed is the same as that of the commanded reference speed. Fig.11 shows the developed torque of the motor. The

starting torque is the rated torque. The steady state torque is about 1 Nm.

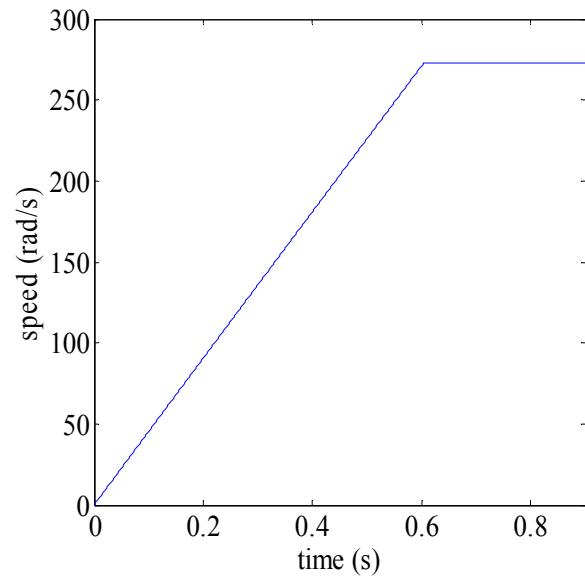


Fig. 10: Dynamic performance for a step variation of the reference speed from 0 RPM to 2600 RPM ($\omega = 272$ rad/s) with a torque load of 1 Nm

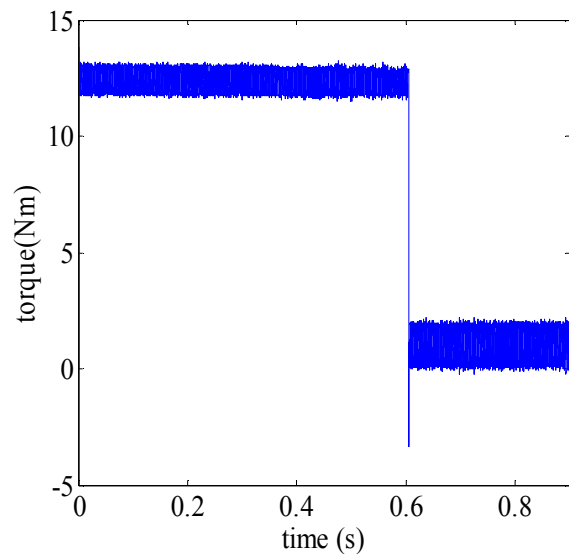


Fig. 11: Developed Torque with Hysteresis Control at 2600 rpm

Fig. 12 shows the real three phase currents drawn by the motor as a result of the hysteresis current control, when the motor changes its speed from -2200 rpm to 2200 rpm with a load torque of 10 Nm. It is clear that the currents are inverted due to the speed variation from -2200 to 2200 rpm. The speed performance is shown in Fig.13 for this case. The steady state speed is the same as that of the commanded reference speed. Fig.14 shows the developed torque of the motor for the speed variation from -2200 to 2200 rpm. The starting torque is the rated torque (12.5 Nm). The steady state torque is about 10 Nm in positive and negative operation of the motor.

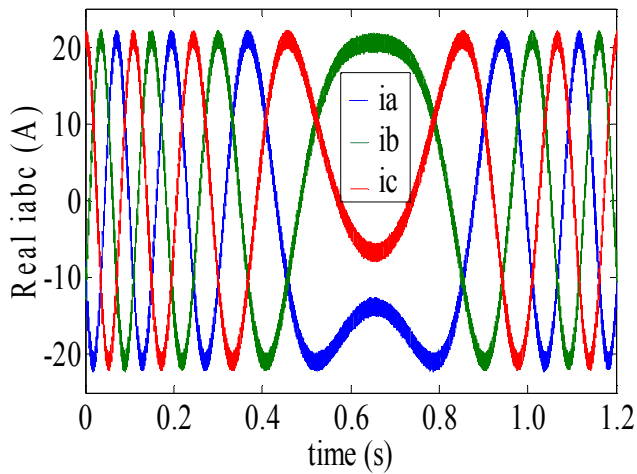


Fig. 12: Inversion of actual phase currents due to a step variation of a speed from -2200 rpm to 2200 rpm ($\omega = 230$ rad/s) with a torque load of 10 Nm

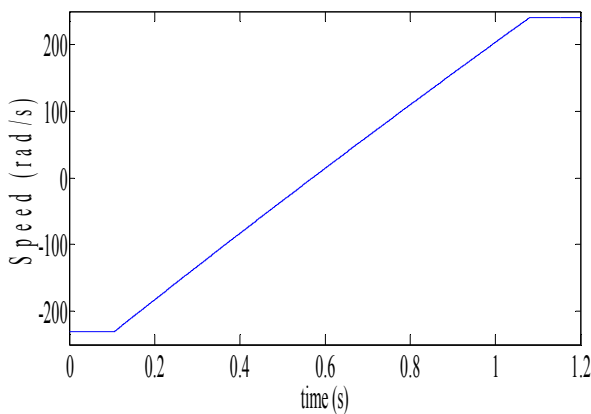


Fig. 13: Dynamic performance for a step variation of the speed from -2200 rpm to 2200 rpm ($\omega = 230$ rad/s) with a torque load of 10 Nm

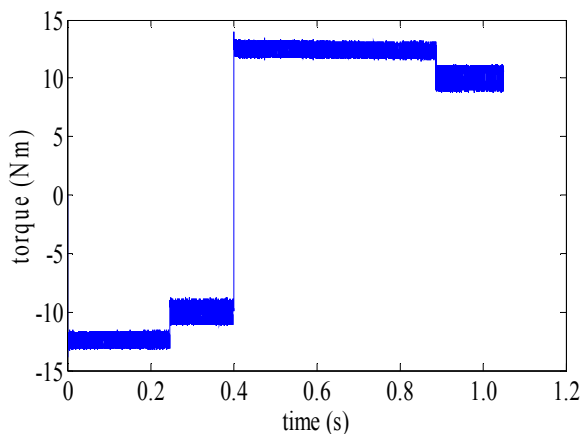


Fig. 14: Developed Torque with Hysteresis Control for a step variation of the speed from -2200 rpm to 2200 rpm ($\omega = 230$ rad/s)

IV. EXPERIMENTAL RESULTS

A DSP based PC board integrated system (TMS320F24X DSP board), is used for vector control of PMSM drive. The schematic diagram of the hardware implementation is shown in Fig. 15. Feedback signals to the controller board are the actual motor currents and the rotor position angle. The currents are measured by the Hall-effect transducers. The currents are then buffered and fed to the A/D ports of the controller board. The motor shaft position is measured by an optical incremental encoder installed at the motor shaft. The commutating signals for the drive pulses have also been generated by the hysteresis controller. The control algorithm has been implemented via the controller board using assembly language programming.

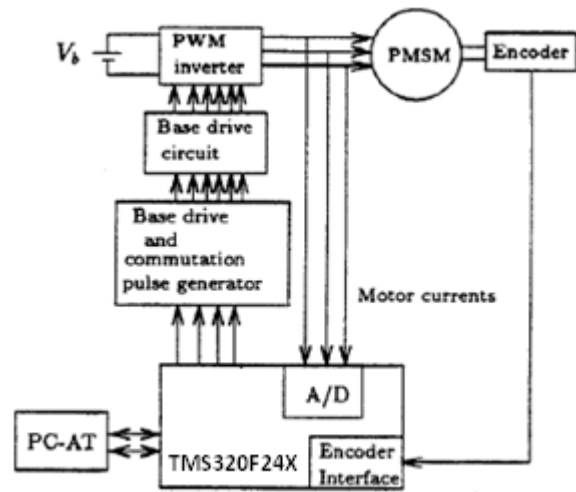


Fig. 15: The hardware schematic of Experimental system

A series of experiments has been carried out to evaluate the performances of the proposed vector controlled PMSM drive system. Different sample results are presented in the following figures. Figs. 16 and 17 demonstrate the actual phase current i_a wave form at different speeds 1500 rpm, 3000rpm respectively.

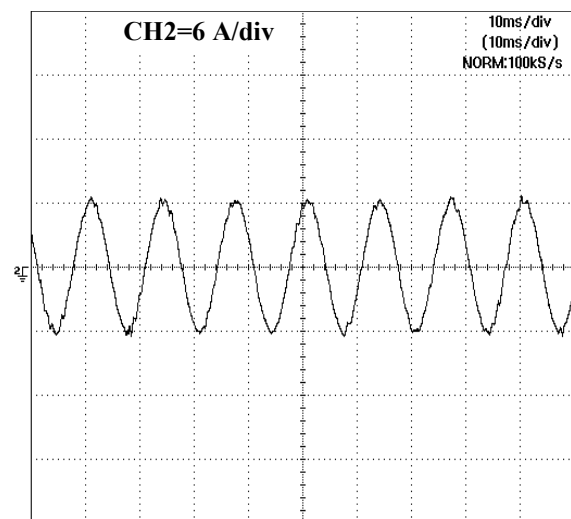


Fig. 16: Actual phase current i_a wave form at 1500 rpm

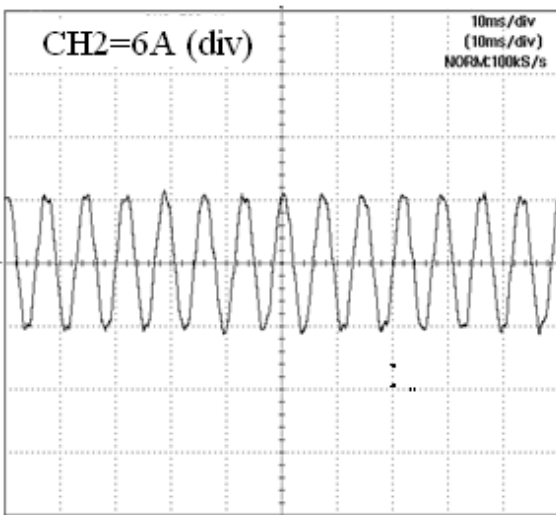


Fig. 17: Actual phase current i_a wave form at 3000 rpm

The experimental evaluation of speed with load as parameter of DSP based PMSM drive is shown in Fig. 18. It shows the step speed response of 2600rpm of the proposed system for a load of 1Nm.

In Fig. 19, the behaviour of the current of phase A is shown during the inversion of speed from 1500 RPM to -1500 rpm with load torque of 11Nm.

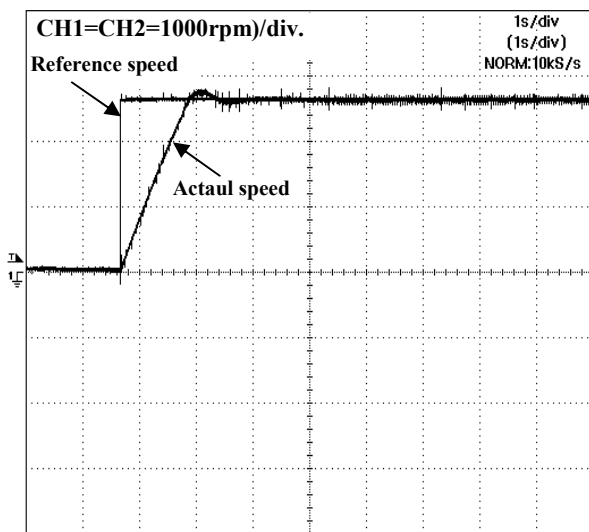


Fig. 18: Experimental speed responses of PMSM drive with step change in load of 1Nm

Fig. 20 shows the response of the drive to a step variation of the reference speed from -2200 to 2200 rpm with a load torque of 1 Nm, the response time is of less than 3s. In Fig. 21, the same experiment is implemented but with a load torque of 10 Nm, the response time is of 3.5s.

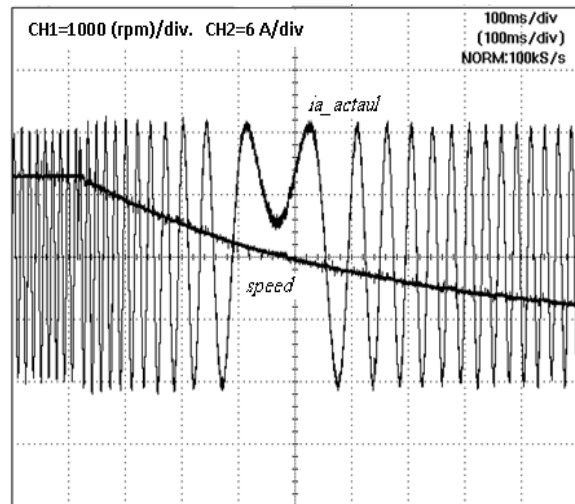


Fig. 19: Inversion of actual speed and actual phase current i_a wave forms due to a step variation of the reference speed from 1500 rpm to -1500 rpm (load Torque of 11 Nm)

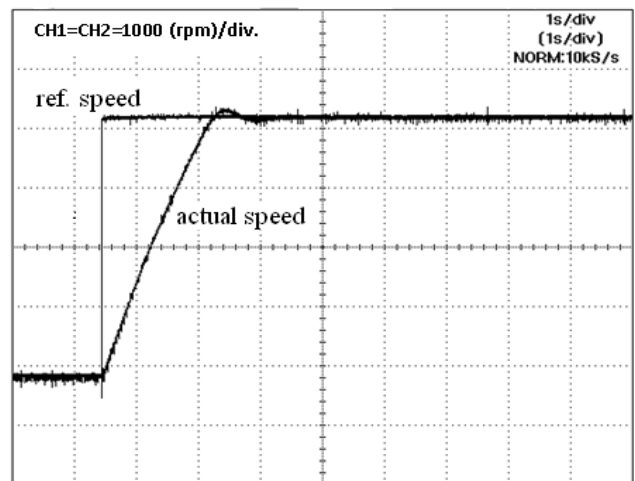


Fig.20: Dynamic performance for a step variation of the reference speed from -2200 rpm to 2200 rpm (load torque of 1 Nm)

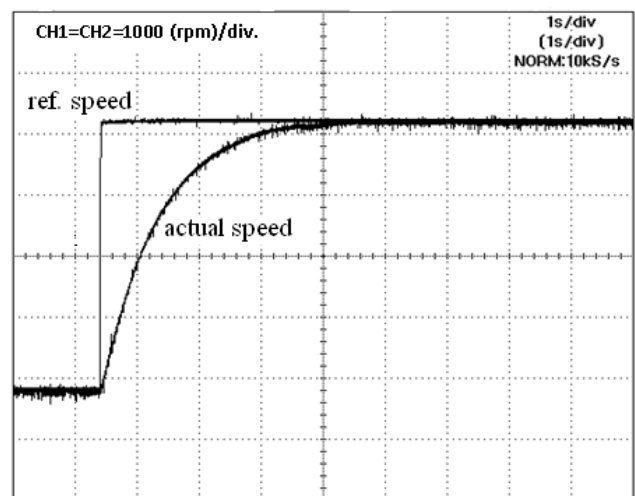


Fig.21: Dynamic performance for a step variation of the speed reference from -2200 rpm to 2200 rpm (load torque of 10 Nm)

V. CONCLUSIONS

The proposed field oriented vector controlled PMSM drive can handle the effects of step change in reference speed and parameter variations. The overall system performances are quite good in terms of dynamic, transient and steady-state responses.

Simulation and experimental results show that the proposed control scheme guarantees stable and robust response of the PMSM drive, under a wide range of operating conditions. Subsequently, it can be utilized in high performance motion control applications.

REFERENCES

- [1] M.H. Rashid, *Power Electronics, Circuits, Devices and Applications*, Pearson Prentice Hall, Upper Saddle River, New Jersey, 2004.
- [2] H.B. Ertan; M.Y. Üctung; R. Colyer; A. Consoli, *Modern Electrical Drives*, Kluwer Academic Publishers, Netherlands, 2000.
- [3] L. Harnefors; P. Taube; H.-P. Nee, An improved method for sensorless adaptive control of permanent-magnet synchronous motors, *Proc. Eur. Conf. Power Electronics*, Trondheim, Vol 4, 1997.
- [4] N. Matsui, Sensorless permanent-magnet brushless DC and synchronous motor drives, *ELECROMOTION*, Vol 3, No. 4, 1996, pp. 172-180.
- [5] A.-K. Daud, Performance analysis of two phase brushless DC motor for sensorless operation, *WSEAS Transactions on Power Systems*, May 2006, Issue 5, Volume 1, pp. 802-809.
- [6] B.-K. Lee; M. Ehsani, Advanced simulation model for brushless dc motor drives, *Electric Power Components and Systems*, September 2003, pp 841-868
- [7] P. Pillay and R. Krishnan, Control characteristics and speed controller design of a high performance PMSM, in *Record IEEE Ind. Appl. Soc. Annu. Meeting.*, 1985, pp. 627-633.
- [8] W. Leonnard, Microcomputer control of high dynamic performance ac drives—a survey, *Automatica*, vol. 22, pp. 1-19, 1986.
- [9] C. Mademlis and N. Margaris, Loss minimization in vector-controlled interior permanent-magnet synchronous motor drives, *Industrial Electronics, IEEE Transactions on*, vol. 49, pp. 1344-1347, 2002.
- [10] X. Jian-Xin, S. K. Panda, P. Ya-Jun, L. Tong Heng, and B. H. Lam, A modular control scheme for PMSM speed control with pulsating torque minimization, *Industrial Electronics, IEEE Transactions on*, vol. 51, pp. 526-536, 2004.
- [11] C.-m. Ong, *Dynamic Simulation of Electric Machinery using Matlab/Simulink*: Prentice Hall, 1998.
- [12] H. Macbahi, A. Ba-razzouk, J. Xu, A. Cheriti, and V. Rajagopalan, A unified method for modeling and simulation of three phase induction motor drives, 2000
- [13] B. K. Bose, *Modern power electronics and AC drives*: Prentice Hall, 2002.
- [14] B. Cui, J. Zhou, and Z. Ren, *Modeling and simulation of permanent magnet synchronous motor drives*, 2001.
- [15] E. Arroyo, *Modeling and simulation of permanent-magnet synchronous motor drive system*, Master of Science in electrical engineering UNIVERSITY OF PUERTO RICO MAYAGÜEZ CAMPUS, 2006.
- [16] Z. Yaou; Z.Wansheng; W.Hongyu, the Study of recursive-based Sliding Mode Adaptive Control of the Permanent Magnet Synchronous Motor, *WSEAS Transactions on Systems*, May 2010, Issue 5, Volume 9, pp. 559-569.
- [17] A. Bara; C. Rusu; S. Dale, DSP application on PMSM drive control for robot axis, *Proceedings of the 13th WSEAS Int. Conf on Systems*, Rodos Island, Greece, July 22-24, 2009, pp. 381-385.
- [18] S. Zhengqiang; H. Zhijian; J. Chuanwen, Sensorless control of surface permanent magnet synchronous motor with a self-adaptive flux observer, *7th WSEAS Int. Conf. on Mathematical Methods and Computational Techniques in Electrical Engineering*, Sofia, 27-29/10/05, pp. 63-68.
- [19] A. Nait Seghir; M.S. Boucherit, Artificial neural network to improve speed control of permanent magnet synchronous motor, *Proceedings of the 6th WSEAS/IASME Int. Conf. on Electric Power Systems, High Voltages, Electric Machines*, Tenerife, Spain, December 16-18, 2006, pp. 94-99.
- [20] Z. Yaou; Z. Wansheng; K. Xiaoming, Control of the Permanent Magnet Synchronous Motor Using Model Reference Dynamic Inversion, *WSEAS TRANSACTIONS on SYSTEMS and CONTROL*, Issue 5, Volume 5, May 2010, pp. 301-311.
- [21] D. Zaltni; M. N. Abdelkrim, Synchronous Motor Observability Study and a New Robust MRAS Speed Observer with an Improved Zero-speed Position Estimation Design for Surface PMSM, *WSEAS TRANSACTIONS on SYSTEMS and CONTROL*, Issue 7, Volume 5, July 2010, pp. 567-580.
- [22] S. J. Dodds; G. Sooriyakumar; R. Perryman, A Robust Forced Dynamic Sliding Mode Minimum Energy Position Controller for Permanent Magnet Synchronous Motor Drives, *WSEAS TRANSACTIONS on SYSTEMS and CONTROL*, Issue 4, Volume 3, April 2008, pp. 299-309.
- [23] E. Hendawi; F. Khater; A. Shaltout, Analysis, Simulation and Implementation of Space Vector Pulse Width Modulation Inverter, *Proceedings of the 9th WSEAS International Conference on Applications of Electrical engineering*, Penang, Malaysia, March 23-25, 2010, pp. 124-131.
- [24] G. K. Dubey, *Fundamentals of electrical drives*, Alpha Science, 2001.